

# Dissolvable Topical Formulations for Burst and Constant Delivery of Vitamin C

Mar Calzado-Delgado, M. Olga Guerrero-Pérez, and King Lun Yeung\*

Cite This: *ACS Omega* 2023, 8, 12636–12643

Read Online

ACCESS |



Metrics &amp; More

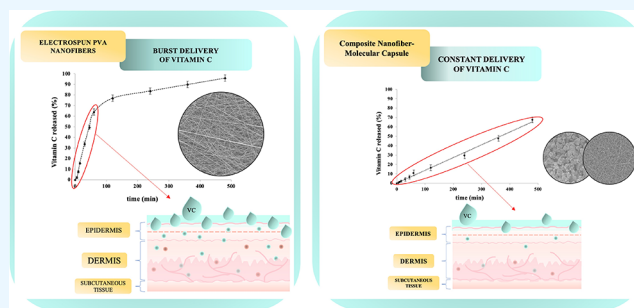


Article Recommendations



Supporting Information

**ABSTRACT:** Healthy skin has a high vitamin C concentration that protects against ultraviolet (UV)-induced damage, promotes wound healing, and lowers cancer risk. The present contribution describes two drug delivery systems for topical administration of vitamin C. The electrospun poly(vinyl alcohol) (PVA) nanofiber carrier of vitamin C exhibits a burst release profile (66 mg/g/h followed by 6.3 mg/g/h). In comparison, a new composite PVA nanofiber–molecular capsule delivers vitamin C at a constant rate (8.2 mg/g/h) with a zeroth-order release profile for better therapeutic management. Both delivery systems protect vitamin C and afford increased heat stability. The molecular capsules of  $\beta$ -cyclodextrin with the vitamin C inclusion complex are immobilized on cellulose acetate and electrospayed onto an electrospun PVA nanofiber mat.



## 1. INTRODUCTION

Vitamin C is an essential nutrient and vital in many biological functions, such as tissue repair, protein synthesis, and iron absorption. A deficiency in vitamin C causes scurvy and the weakening of connecting tissues and blood capillaries.<sup>1</sup> In addition, it possesses several antioxidant properties, neutralizes free radicals within and outside the cells, and is beneficial against common cold, cataracts, age-related muscular degeneration, cardiovascular diseases, and some types of cancer.<sup>2–4</sup> Moreover, vitamin C keeps skin healthy by protecting it from UV-induced damage, promotes wound healing, and decreases skin cancer risk.<sup>5</sup> Indeed, healthy skin is rich in vitamin C with 60–640 mg/g in the epidermis and 30–130 mg/g in the dermis and are reported decreases in aged and photodamaged skin due to lower vitamin C levels in blood plasma.<sup>6,7</sup>

The topical application delivers vitamin C directly to the epidermal layer and replenishes the skin.<sup>8,9</sup> However, the efficacy depends on the formulation of vitamin C as the stratum corneum repels water-soluble and charged molecules. In addition, a low pH is required to facilitate penetrations, which causes skin sensitivity and irritation. Thus, several approaches have been explored as vitamin C carriers, including solid lipids,<sup>10</sup> liposomes,<sup>11</sup> and polymeric nanoparticles<sup>12</sup> that slowly release vitamin C allowing greater uptake. Indeed, nanoparticle carriers with tumor-receptors can specifically target and deliver vitamin C to tumor sites.<sup>13</sup> There are, however, numerous shortcomings, most notably the cost and stability of these formulations. One approach that seems to be promising for delivering vitamin C is the use of electrospun dissolvable polymer nanofibers as a carrier to control the release and delivery on the skin, since electrospun nanofibers

have been explored for modifying several drug release profiles such as pulsatile, sustained, or targeted release, and even for biphasic release.<sup>14,15</sup>

The electrospun PVA material exhibits a burst release profile typical of most of the polymeric systems. But with a combination of electrospinning and electrospaying, a novel composite PVA nanofiber–molecular capsule will be prepared, giving a zeroth-order release profile, which follows a suitable and controllable delivery of vitamin C over time and can fit for better therapeutic applications. In this manner, the new material proposed can be incorporated to a skin patch that would start working once it is in contact with the skin's moisture, releasing vitamin C as a controllable and linear release over time.

Highly reproducible electrospun nanofiber patches were made using a newly designed versatile electrospinning equipment that provides a rapid and precise *x-y-z* movement and accurate positioning.<sup>16</sup> Furthermore, the fiber diameter, mesh morphology, and layer thickness are accurately controlled to produce multilayered patches and composite nanofiber–molecular capsule patches for storing vitamin C for controlled release experiments.

Received: October 19, 2022

Accepted: December 14, 2022

Published: March 27, 2023



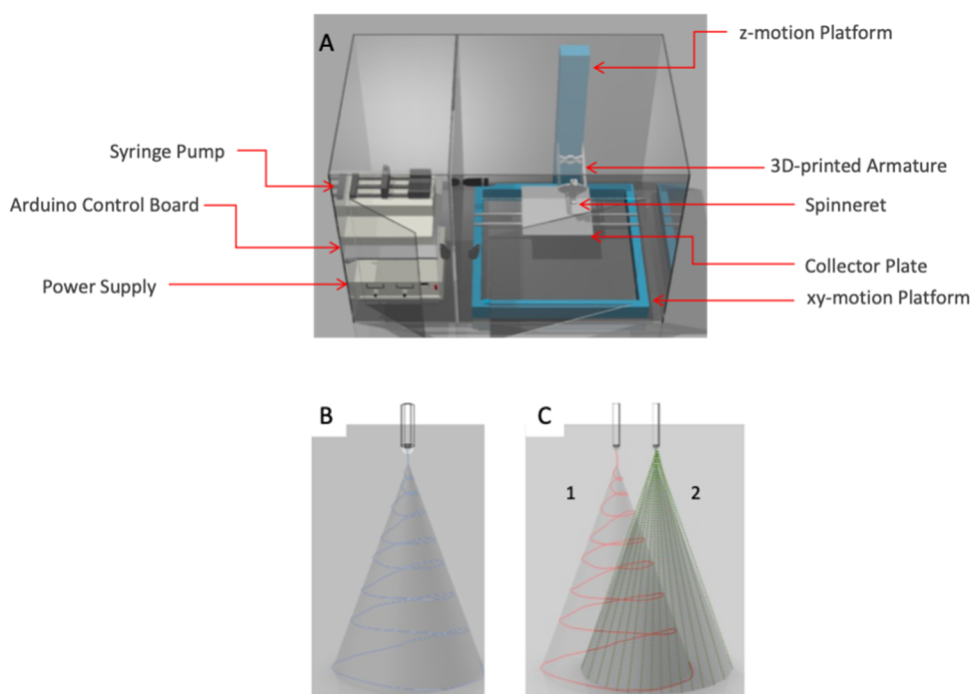


**Figure 1.** (A) Schematic drawing of the new versatile  $x$ - $y$ - $z$  electrospinning equipment<sup>13</sup> and illustrations of (B) the electrospinning of the nanofiber carrier for vitamin C and (C) composite nanofiber–molecular capsule of vitamin C via sequential electrospinning (1) and electro spraying (2) processes.

## 2. EXPERIMENTAL METHODS

### 2.1. Preparation of the Nanofiber Carrier for Vitamin C

The poly(vinyl alcohol) (PVA, MW: 40,000–70,000, 98% hydrolyzed) supplied by Sigma-Aldrich was slowly dissolved in 80 °C distilled deionized (DDI) water over 2 h to obtain a 15 w/v % PVA solution. After cooling to room temperature, vitamin C (*L*-ascorbic acid) was added to the clear homogeneous solution to give a 10 wt % loading based on the polymer weight. The solution was transferred to the electrospinning equipment (Figure 1A), and the vitamin C-loaded PVA nanofiber was electrospun from a 210  $\mu\text{m}$  spinneret needle at a 10.6 kV and a needle-to-collector distance of 13 cm (Figure 1B). The polymer flow was kept at 0.1 mL/h, and the nanofiber was collected on aluminum. All reagents are biocompatible and nontoxic in the dosage that they were prepared and used.<sup>17,18</sup>

**2.2. Preparation of the Composite Nanofiber–Molecular Capsule for Vitamin C.** The molecular capsule of vitamin C was prepared by storing vitamin C in  $\beta$ -cyclodextrin ( $\beta$ -CyD) and dispersing the capsules on a cellulose acetate carrier. Briefly,  $\beta$ -CyD (>97%) from Sigma-Aldrich was dissolved in 33 v/v % ethanol in DDI water at 55 °C to obtain 10 wt %  $\beta$ -CyD. Vitamin C was then slowly added to give a 1:1 molar ratio of vitamin C to  $\beta$ -CyD. Afterward, the solution was cooled to room temperature with constant stirring for over 4 h before storing at 5 °C for another 12 h. It was followed by filtration and washing with ethanol to remove excess vitamin C before drying in vacuum at 50 °C for 12 h; 3% (w/v) of cellulose acetate (CA, MW: 50,000) purchased from Sigma-Aldrich was dissolved in 3 dichloromethane (AR, RCI Labscan)/1 ethanol (absolute, Scharlau) solution to which 5% (w/v) of vitamin C-loaded  $\beta$ -CyD was added and stirred to obtain a homogeneous solution for electro spraying onto a PVA nanofiber mat.

The PVA nanofiber mat was electrospun from a 10 w/v % PVA solution. The solution was obtained by dissolving PVA (MW: 125,000, Mowiol 20–98) from Sigma-Aldrich in DDI water at 90 °C. The solution remains homogeneous after cooling to room temperature. The electrospinning process was performed at 7.3 kV, a needle-to-collector distance of 13 cm, and a polymer flow of 0.1 mL/h. The PVA nanofibers were then electro sprayed with the prepared molecular capsules of vitamin C at 10.5 kV, a needle-to-collector distance of 15 cm, and a solution flow of 0.7 mL/h. (Figure 1C) to obtain the composite nanofiber–molecular capsule of vitamin C.

**2.3. Characterization of the Nanofiber Carrier and Composite Nanofiber–Molecular Capsule.** Samples were observed under a scanning electron microscope (JEOL JSM-7100F), and the nanofiber and particle diameters were measured using ImageJ and processed using IBM SPSS Statistics 23 software. The samples were also analyzed by a Bruker Vertex 70 Hyperion 1000 Fourier transform infrared spectrometer by adding 86 scans in the 4000–400  $\text{cm}^{-1}$  spectral range at a 4  $\text{cm}^{-1}$  resolution.<sup>19</sup> Moreover, thermogravimetric analysis was done on a Perkin Elmer UNIX/TGA7 at a 5 °C/min heating rate from room temperature to 800 °C in 40 sccm dry air.

The loading efficiency (LE%) of vitamin C was calculated from the theoretical loading percentage (TLP%) and loading percentage (LP %). TLP and LP values were determined by dissolving the carrier and analyzing the vitamin C content using an ultraviolet–visible (UV–vis) spectrophotometer. For example, 13 mg of vitamin C-loaded  $\beta$ -CyD was dissolved in 20 mL of 1% of the oxalic acid solution for 24 h, and the vitamin C content was measured by a Cary 3500 UV–vis spectrophotometer. Thus, LE% was calculated from eqs 1–3

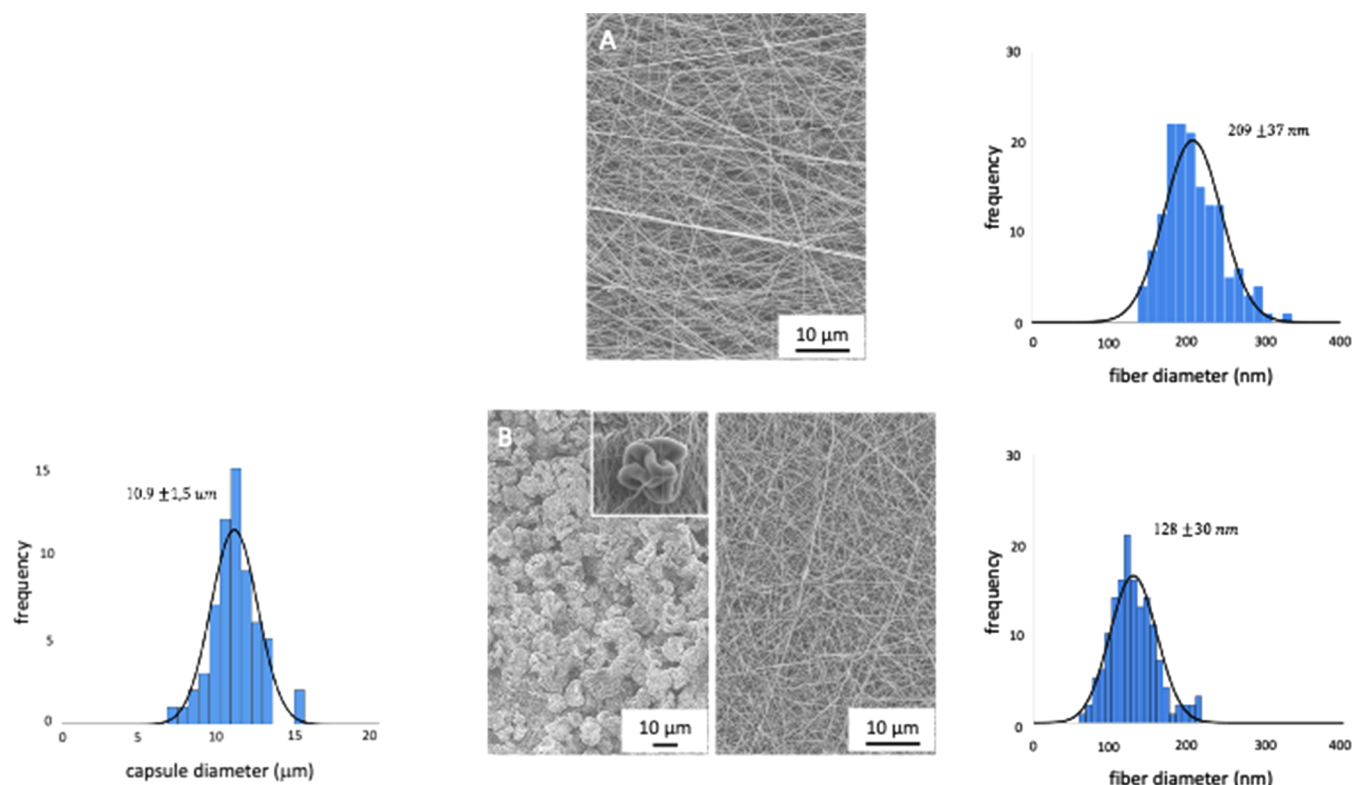


**Figure 2.** Scanning electron microscopy images and size distribution of (A) the  $209 \pm 37$  nm PVA nanofiber carrier of vitamin C and (B) the composite nanofiber–molecular capsule of vitamin C where the left-hand image of the image is the CA- $\beta$ CD capsules of vitamin C (inset: a high magnification image of the  $10.9 \pm 1.5$   $\mu\text{m}$  particle) and the right-hand image of the  $128 \pm 30$  nm PVA nanofiber substrate.

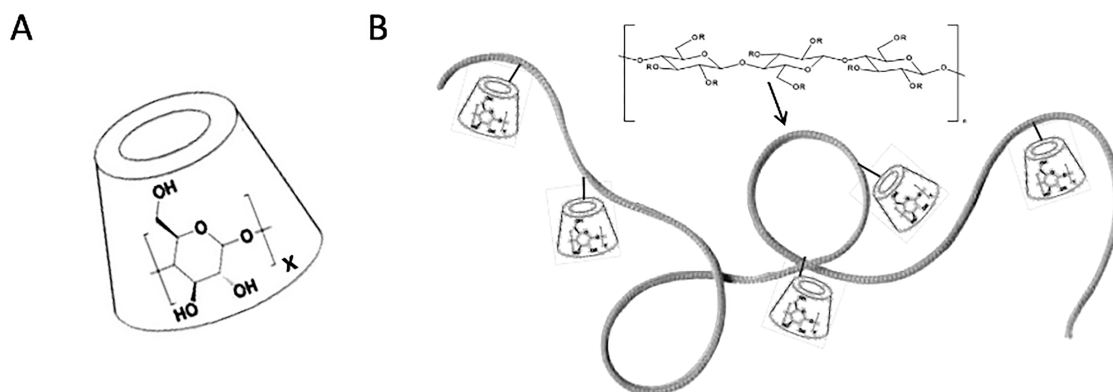


**Figure 3.** Schematic drawings of (A) the vitamin C-loaded  $\beta$ CD molecular capsule and (B) CA- $\beta$ CD capsule where the vitamin C-loaded  $\beta$ CD capsules are dispersed and immobilized on CA polymeric strands.

$$\text{LP\%} = \frac{\text{mass of encapsulated vitamin C}}{\text{mass of vitamin C} + \beta\text{CyD (complex)}} \times 100 \quad (1)$$

$$\text{TLP\%} = \frac{\text{mass of vitamin C in the solution}}{\text{total mass of vitamin C and } \beta\text{CyD in the solution (complex)}} \times 100 \quad (2)$$

$$\text{LE\%} = \frac{\text{actual loading percentage (LP)}}{\text{theoretical loading percentage (TLP)}} \times 100 \quad (3)$$

**2.4. Vitamin C Release Profile and Rate.** An *in vitro* release experiment was conducted by immersing 45 mg samples of the nanofiber vitamin C carrier and 65 mg of composite nanofiber–molecule capsules of vitamin C in 25 mL

of phosphate buffer saline (PBS) solution kept at  $37$   $^{\circ}\text{C}$  and under continuous 100 rpm mixing. Aliquots were taken at fixed intervals over 8 h and analyzed by a UV–vis spectrophotometer. The drug release mechanism was fitted against different models.<sup>20</sup> Zeroth-order release kinetics (cf. eq 4) with a constant dosing rate is preferred as it provides manageable treatment, while the most common release rate is the first-order and nonlinear (eq 5). The Hixson–Crowell model (eq 6) describes the release of drugs from shrinking and swelling carriers exhibiting a change in the exposed surface area.<sup>21,22</sup> The Korsmeyer–Peppas model (eq 7) describes a Fickian model for drug diffusion for  $n < 0.45$ , irregular transport for  $0.45 < n < 1$ , zeroth order for  $n = 1$ , and super Case-II transport for  $n > 1$ .

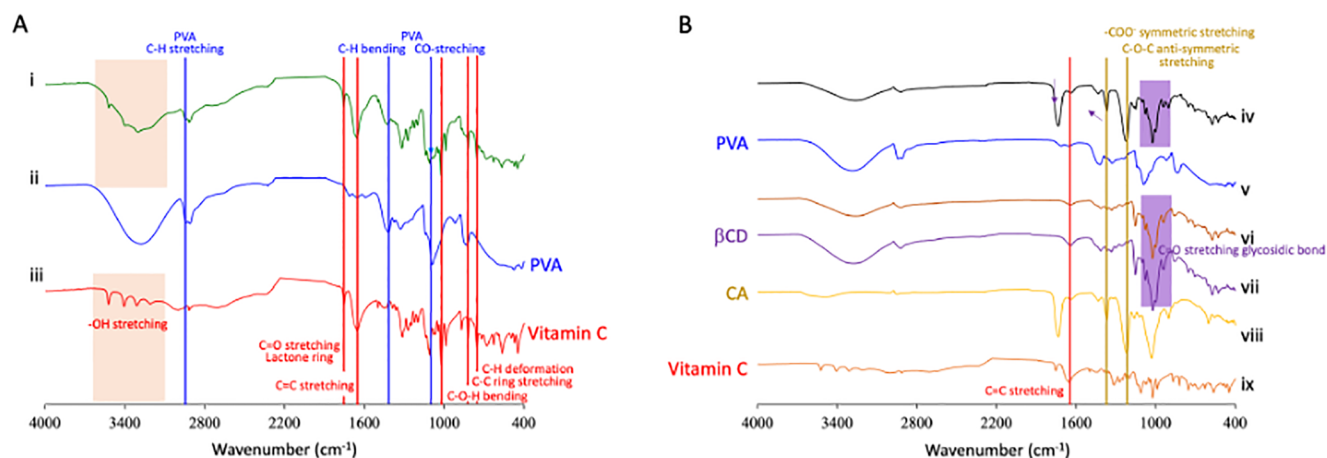


**Figure 4.** FTIR spectra of (A) the PVA nanofiber carrier of vitamin C: (i) vitamin C-loaded PVA nanofiber carrier, (ii) PVA nanofiber, and (iii) vitamin C and (B) composite nanofiber–molecular capsules of vitamin C: (iv) vitamin C-loaded CA- $\beta$ CD capsules electrospun on the electrospun PVA nanofiber, (v) PVA nanofiber, (vi) vitamin C-loaded  $\beta$ CD molecular capsules, (vii)  $\beta$ CD, (viii) CA, and (ix) vitamin C.

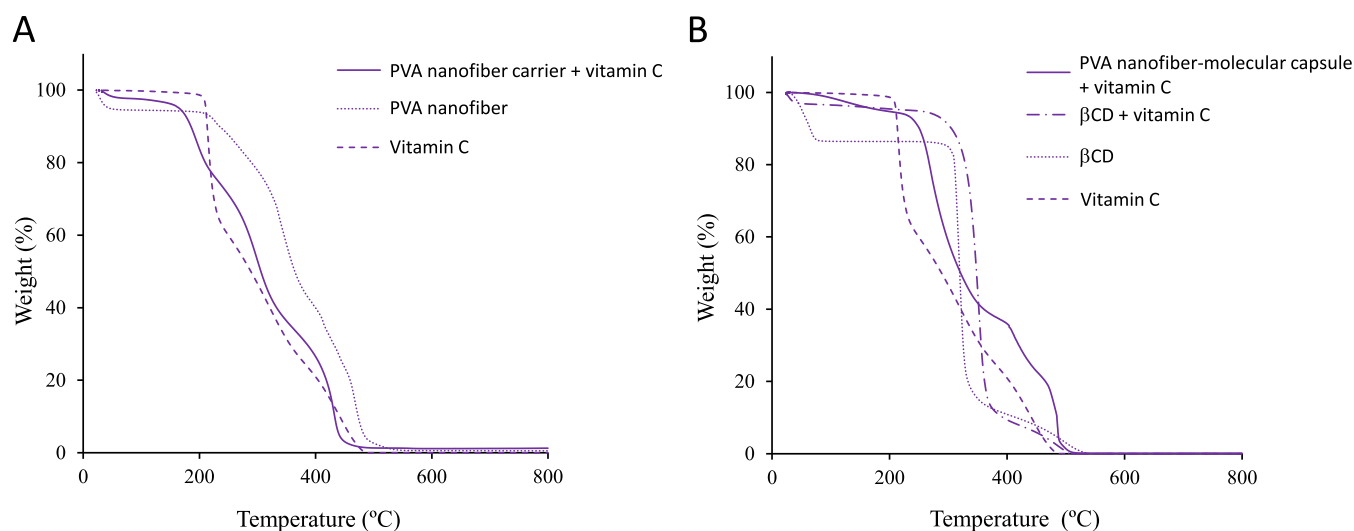


**Figure 5.** Thermogravimetric analysis of (A) the PVA nanofiber carrier loaded with vitamin C and (B) the composite PVA nanofiber–molecular capsule of vitamin C. TGA of the PVA nanofiber, vitamin C, vitamin C-loaded  $\beta$ CD, and  $\beta$ CD are included for comparison.

$$M_t = M_0 + k_0 t \quad (4)$$

$$\log M_t = \log M_0 - \frac{k_1}{2.303} t \quad (5)$$

$$M_\infty^{1/3} - M_t^{1/3} = kt \quad (6)$$

$$\frac{M_t}{M_\infty} = k_{kp} t^n \quad (7)$$

where  $M_0$  is the initial concentration of vitamin C in the solution,  $M_t$  is the concentration of vitamin at time  $t$ ,  $M_\infty$  is the equilibrium concentration of vitamin C,  $k_0$  is the rate constant for the zeroth-order release kinetics,  $k_1$  is the first-order release kinetics,  $k_{kp}$  is the Korsmeyer–Peppas rate constant with  $n$  being the exponent of release.<sup>23</sup>

### 3. RESULTS AND DISCUSSION

The nanofiber carrier and composite nanofiber–molecular capsules of vitamin C were observed under a SEM and presented in Figure 2 with a size distribution of the fiber and

capsule diameters. The PVA nanofibers loaded with vitamin C shown in Figure 2A have a coarser diameter (i.e.,  $209 \pm 37$  nm) and the PVA nanofibers (i.e.,  $128 \pm 30$  nm) without vitamin C are shown in cf. Figure 2B-right. The vitamin C loading was 10 wt % of the electrospun polymer weight.

The composite nanofiber–molecular capsule of vitamin C is shown in Figure 2B. The left-hand SEM image shows the sample's surface deposited with a layer of uniform  $10.9 \pm 1.5$   $\mu$ m of CA- $\beta$ CD capsules of vitamin C (cf. Figure 2B-left inset). The vitamin was loaded within the  $\beta$ CD molecular capsules (Figure 3A), and the capsules were, in turn, immobilized on cellulose acetate polymer (Figure 3B) to create the micron-size particles as shown in the figure. The supporting PVA nanofiber mat is presented in Figure 2B-right.

The FTIR spectrum of the PVA nanofiber carrier of vitamin C is presented in Figure 4A, along with the spectra of electrospun PVA nanofibers and vitamin C. Identifying the characteristic bands of PVA and vitamin C on the sample is possible. These include the CO-stretching ( $1093$   $\text{cm}^{-1}$ ), CH-bending ( $1420$   $\text{cm}^{-1}$ ), and C–H stretching ( $2941$   $\text{cm}^{-1}$ ) from PVA<sup>24</sup> and the C–H deformation ( $754$   $\text{cm}^{-1}$ ), C–C ring

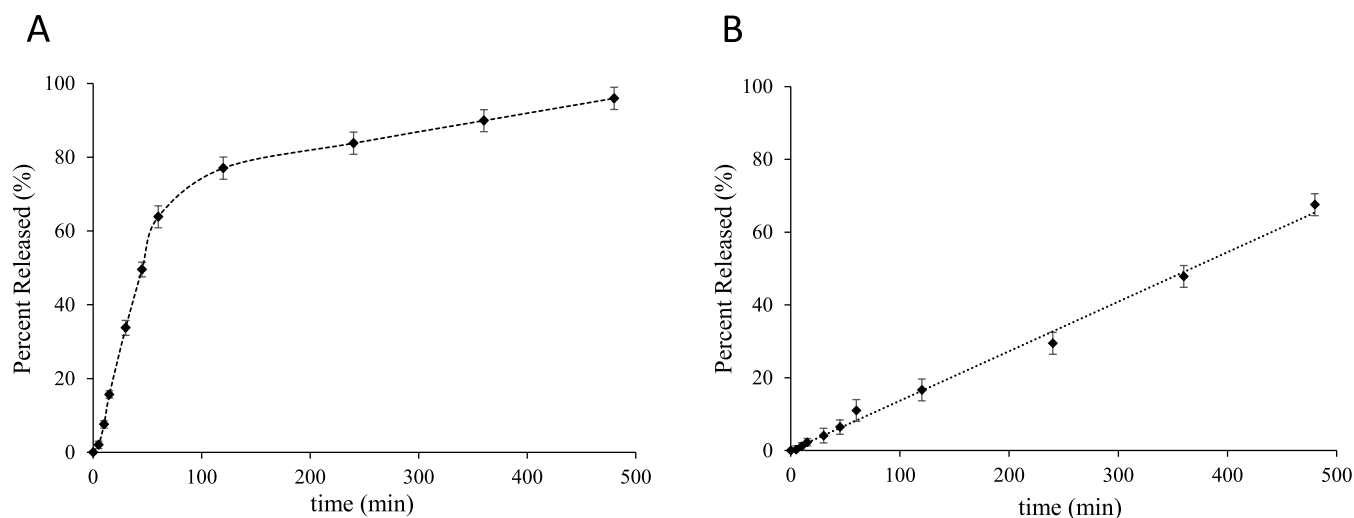


**Figure 6.** Plots of vitamin C released from (A) the nanofiber carrier and (B) composite nanofiber–molecular capsules containing 10 wt % vitamin C. Note: PBS solution at 37 °C and 8 h.

stretching ( $867\text{ cm}^{-1}$ ), C–O–H bending ( $1022\text{ cm}^{-1}$ ), C=C stretching ( $1651\text{ cm}^{-1}$ ), lactone ring C=O stretching ( $1750\text{ cm}^{-1}$ ), and weak peaks from –OH stretching (ca.  $3200\text{--}3600\text{ cm}^{-1}$ ) belonging to vitamin C. It is important to note that the PVA's C–O band at  $1690\text{ cm}^{-1}$  from residual acetate is very weak, confirming that it was fully hydrolyzed. Vitamin C also presents a band at ( $1317\text{ cm}^{-1}$ ) from the enol-hydroxyl bond that is also present in the sample.<sup>25</sup>

Figure 4B presents the FTIR spectra of the front (iv) and back (v) of the composite nanofiber–molecular capsule of vitamin C. The uniform layer of CA- $\beta$ CD capsules of vitamin C (Figure 2B-left) presents bands originating from vitamin C (ix),  $\beta$ CD (vii), CA (viii), and a few weak bands from PVA (v).<sup>26</sup> These are the C=C stretching ( $1651\text{ cm}^{-1}$ ) belonging to vitamin C, glycosidic C=O stretchings ( $1026\text{ cm}^{-1}$ ) from  $\beta$ CD, and the C–O–C symmetric stretching ( $1240\text{ cm}^{-1}$ ) and –COO<sup>–</sup> symmetric stretching ( $1371\text{ cm}^{-1}$ ) from CA. The C–O stretching band from PVA is barely discernible from the front side of the sample. The back of the sample is purely PVA (Figure 4B-(iv)), indicating that the CA- $\beta$ CD capsules loaded with vitamin C are only deposited on the front side of the sample.

The FTIR spectra in Figure 4A indicate that vitamin C has weak interactions with PVA as deduced from the distinct –OH stretching bands from vitamin C loaded in the PVA nanofiber carrier. A prior study showed that  $\beta$ CD and vitamin C form a thermodynamically stable 1:1 host–guest complex in an aqueous solution.<sup>27</sup> It was determined that the nonpolar part of vitamin C is hosted within the  $\beta$ CD cavity, while the polar groups are stabilized through hydrogen-bond interactions with the hydroxyl groups surrounding the  $\beta$ CD's polar rims. After loading vitamin C into  $\beta$ CD, the –OH stretching bands disappeared, possibly from the formation of hydrogen bonding, and the only distinguishing peak is the band at  $1640\text{ cm}^{-1}$  attributed to the C=C stretching in vitamin C (Figure 4B-(vi)). Dispersing the molecular capsules on CA results in the disappearance of  $858\text{ cm}^{-1}$  and the appearance of  $902\text{ cm}^{-1}$  band that is attributed to the C–O–C stretching of the glucose unit after attaching  $\beta$ CD to CA.

Thermogravimetric analysis of the nanofiber carrier and composite nanofiber–molecular capsules are reported in Figure 5. Figure 5A shows that the PVA nanofiber and vitamin

C are stable up to 200 °C in air. Indeed, PVA is reported to protect vitamin C from degradation and preserve its bioactivity.<sup>28</sup> The vitamin C-loaded nanofiber carrier tolerates up to 180 °C heating before showing significant dehydration. It is slightly more heat-stable than vitamin C but cannot tolerate heating, as well as the pure PVA nanofiber. It is caused by the formation of noncovalent bonds between vitamin C and PVA, weakening the bonds between polymers. Loading vitamin C into  $\beta$ CD allows it to withstand heating to 350 °C (Figure 5B) due to the formation of the host–guest inclusion complex.  $\beta$ CD displays weight loss (ca. 16%) from dehydration when heated to 100 °C. The formation of the vitamin C inclusion complex releases water molecules from the hydrophobic cavity of  $\beta$ CD. Hence, it is unsurprising that vitamin C-loaded  $\beta$ CD suffered less than 5% weight loss by dehydration. Also, immobilizing  $\beta$ CD on CA forms covalent bonds through condensation reactions, further decreasing the water content of the material. The composite nanofiber–molecular capsule displays better stability than vitamin C and the PVA nanofiber.

PVA is considered a versatile material for drug delivery, wound dressing, and tissue engineering, having superb biocompatibility and excellent thermomechanical properties.<sup>29</sup> In addition, it is readily soluble in water and biodegradable enabling safe, clean, and sustainable preparation and processing. Figure 6 plots vitamin C release from the nanofiber carrier (Figure 6A) and composite nanofiber–molecular capsule (Figure 6B). The vitamin C release from the PVA nanofiber carrier is nonlinear, with a rapid release rate of 1.1 mg/g/min (66 mg/g/h) during the first 60 minutes and roughly 63% of the vitamin C load in the process. Then, a slower release rate of 6.3 mg/g/h until 96% of the vitamin C was released after 48 h. The initial burst release is common in many drug delivery systems<sup>30</sup> and in PVA this is ascribed to the hydrosweeling of the polymer. It is then followed by slow degradation of water-soluble PVA releasing the remaining vitamin C from the nanofiber carrier. Burst release of vitamin C immediately lowers the pH facilitating its skin penetration. However, it could cause skin irritation and in severe cases, skin sensitization and dermatitis.

The release profile of vitamin C from the PVA nanofiber carrier best fits the Hixon–Crowell model (Table 1), where the drug release rate depends on the carriers' surface area.

**Table 1. Model Fitting for the Vitamin C Release Rate**

model	parameter	samples	
		nanofiber carrier	composite nanofiber–molecular capsules
zeroth order	$k$	64.3	8.16
	$R^2$	0.993	0.999
first order	$k$	0.970	0.127
	$R^2$	0.990	0.963
Hixon–Crowell	$k$	21.4	2.72
	$R^2$	0.995	0.995
Korsmeyer–Peppas	$k$	74.4	7.67
	$R^2$	0.974	0.973
	$n$	1.35	1.10

Indeed, the vitamin C-loaded PVA nanofiber carrier swelled once in contact with water altering the fiber area and vitamin C concentration within the nanofibers. The PVA nanofiber dissolution was observed beyond an hour of immersion in water with the disappearance of the nanofiber structure and formation of an amorphous film. The latter results in an enormous loss of surface area that would retard vitamin C release, as observed in Figure 6A.

$\beta$ -Cyclodextrin, according to the U.S. Food and Drug Administration (FDA), is “generally recognized as safe” (GRAS) for food additives, and its topical toxicity has been well studied.<sup>31</sup> In addition, it is safe for skin applications, including transdermal drug delivery, skin protection, and cosmetic applications.<sup>32,33</sup> Cyclodextrin often enhances the stability and solubility of drugs in topical formulations while controlling their release and promoting their absorption. Although cyclodextrin interacts with stratum corneum’s lipids, thus creating a pathway for drug penetration, it has low percutaneous penetration and avoids potential side effects.<sup>34</sup> The controlled drug delivery research is driven by the quest for a controlled zeroth-order drug release kinetics.<sup>35</sup> Zeroth-order release kinetics is essential to keep drug concentrations within the therapeutic range between the minimum effective concentration and below the maximum toxic concentration. However, the zeroth-order release rate is rare, and most drug

release profiles are nonlinear, with triphasic release profiles being the most common. Figure 6B shows that the composite nanofiber–molecular capsule releases vitamin C at a constant rate of 8.2 mg/g/h and has a zeroth-order kinetic rate for better therapeutic management. It is achieved using  $\beta$ CD to create a stable vitamin C inclusion complex and immobilizing these molecular capsules on CA to moderate the hydration level and control the displacement of vitamin C from the  $\beta$ CD cavity. Thus, it is possible to control the release rate by managing the loading of molecular capsules on CA.

These release experiments agree with the chemistry observed under FTIR (Figure 4). The weak interaction of vitamin C with PVA chains resulted in the fast burst release of vitamin C from the PVA nanofiber carrier (Figure 7A). Vitamin C diffuses from the swollen PVA chains, and the process is accompanied by a significant change in the nanofiber morphology and surface area. On the other hand, the stronger molecular interactions between vitamin C and the  $\beta$ CD host gave a more controllable release of vitamin C. The release occurs as water displaces the hydrogen bonding between vitamin C and the hydroxyl groups surrounding the lip of the capsule. Thus, controlling the hydration using cellulose acetate, the release could be adjusted to give a zeroth-order dosing rate over an extended period, as shown in Figure 7B.

#### 4. CONCLUSIONS

Two topical vitamin C delivery systems were investigated. Both delivery systems protect vitamin C and increase their heat resistance. The PVA nanofiber carrier displays typical nonlinear burst release profile with an initial rapid release of 66 mg of vitamin C/g/h triggered by the rapid swelling of the nanofiber in water. It was then followed by a slow-release rate (6.3 mg/g/h) with the dissolution of the nanofiber and formation of a dense film. Vitamin C is believed to be the causative factor in the nanofiber dissolution as it forms noncovalent bonds with PVA, thus weakening the bonds between polymers. The release kinetics is best described by the Hixon–Crowell model. The second delivery system consists of CA-immobilized  $\beta$ CD molecular capsules loaded with the vitamin C inclusion complex electrospayed on a PVA

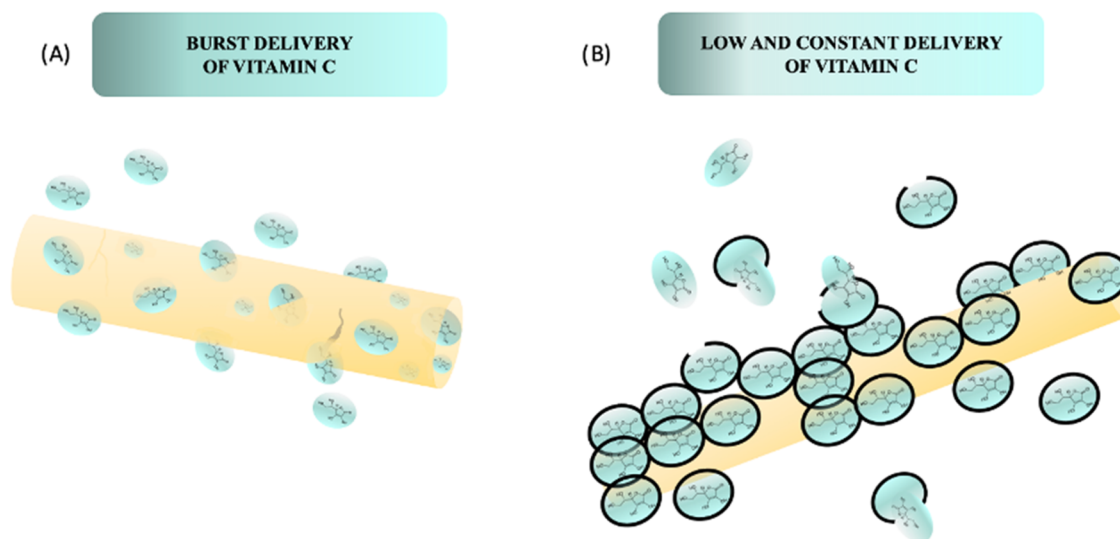


**Figure 7.** Proposed vitamin delivery mechanisms from (A) the burst release from PVA nanofibers and (B) constant dosing from the composite nanofiber–molecular capsules.

nanofiber mat. The composite nanofiber–molecular capsule releases vitamin C at a constant rate with a zeroth-order release profile that is critical in therapeutic management. A judicious combination of the two delivery systems can create programmable release profiles from the zeroth-order, constant release rate to the nonlinear burst, biphasic, and triphasic release profiles to cover a broad range of therapeutic needs. By this manner, the CA-immobilized  $\beta$ CD molecular capsules loaded with vitamin C materials could be incorporated to a skin patch that would start working once it is in contact with the skin's moisture, releasing vitamin C as a controllable and linear release over time.

## ■ ASSOCIATED CONTENT

### SI Supporting Information

The Supporting Information is available free of charge at <https://pubs.acs.org/doi/10.1021/acsomega.2c06738>.

Main functional groups present in cellulose acetate (CA),  $\beta$ -cyclodextrin ( $\beta$ CD), vitamin C (Vc), and polyvinyl alcohol (PVA); characteristic IR absorption frequencies for pure PVA and Vc; characteristic IR absorption frequencies for  $\beta$ CD and CA (PDF)

## ■ AUTHOR INFORMATION

### Corresponding Author

**King Lun Yeung** – Department of Chemical and Biological Engineering, The Hong Kong University of Science and Technology, Kowloon 999077 Hong Kong, P. R. China; Division of Environment and Sustainability, The Hong Kong University of Science and Technology, Kowloon 999077 Hong Kong, P. R. China; HKUST Shenzhen-Hong Kong Collaborative Innovation Research Institute, Shenzhen 518000 Guangdong, P. R. China; [orcid.org/0000-0002-6970-8483](https://orcid.org/0000-0002-6970-8483); Email: [kekyeung@ust.hk](mailto:kekyeung@ust.hk)

### Authors

**Mar Calzado-Delgado** – Department of Chemical and Biological Engineering, The Hong Kong University of Science and Technology, Kowloon 999077 Hong Kong, P. R. China; Department of Chemical Engineering, University de Málaga, E29071 Málaga, Spain

**M. Olga Guerrero-Pérez** – Department of Chemical Engineering, University de Málaga, E29071 Málaga, Spain; [orcid.org/0000-0002-3786-5839](https://orcid.org/0000-0002-3786-5839)

Complete contact information is available at: <https://pubs.acs.org/doi/10.1021/acsomega.2c06738>

### Author Contributions

M.C.D., M.O.G.P., and K.L.Y. contributed to the analysis, discussion, and preparation of the manuscript; M.C.D. conducted the experimental studies under the supervision of K.L.Y. and M.O.G.P.; and K.L.Y. is the principal investigator of the research funding.

### Notes

The authors declare no competing financial interest.

## ■ ACKNOWLEDGMENTS

The authors gratefully acknowledge financial support from the European Union-Hong Kong Research and Innovation Cooperation Co-Funding Mechanism (E-HKUST601/17) from the Hong Kong Research Grants Council and the European Union's Horizon 2020 (BIORIMA). This work is

supported in part by the Project of the Hetao Shenzhen-Hong Kong Science and Technology Innovation Cooperation Zone (HZQB-KCZYB-2020083). In addition, M.C.D. appreciates the award of an Erasmus Mundus Action 2 Strand 2 (EMA2/S2 EurasiaCat) scholarship for her stay in Hong Kong and the Postgraduate Studentship Award from The Hong Kong University of Science and Technology. The authors also thank Y. Huang and M. Zhu for their help in conducting the FTIR and TGA measurements and in participating in the vitamin C release experiments.

## ■ ABBREVIATIONS

PVA, poly(vinyl alcohol); CA, cellulose acetate;  $\beta$ CD,  $\beta$ -cyclodextrin; DDI water, distilled deionized water; SEM, scanning electron microscopy; TGA, thermogravimetric analysis; FTIR, Fourier transform infrared spectroscopy; PBS, phosphate buffer saline

## ■ REFERENCES

- (1) Buckley, H. R.; Kinaston, R.; Halcrow, S. E.; Foster, A.; Spriggs, M.; Bedford, S. Scurvy in a tropical paradise? Evaluating the possibility of infant and adult vitamin C deficiency in the Lapita skeletal sample of Teouma, Vanuatu, Pacific islands. *Int. J. Paleopathol.* **2014**, *5*, 72–85.
- (2) Lim, J. C.; Arredondo, M. C.; Braakhuis, A. J.; Donaldson, P. J. Vitamin C and the Lens: New Insights into Delaying the Onset of Cataract. *Nutrients* **2020**, *12*, No. 3142.
- (3) Moser, M. A.; Chun, O. K. Vitamin C and Heart Health: A Review Based on Findings from Epidemiologic Studies. *Int. J. Mol. Sci.* **2016**, *17*, No. 1328.
- (4) Du, J.; Cullen, J. J.; Buettner, G. R. Ascorbic acid: Chemistry, biology and the treatment of cancer. *Biochim. Biophys. Acta, Rev. Cancer* **2012**, *1826*, 443–457.
- (5) Pullar, J. M.; Carr, A. C.; Vissers, M. C. M. The Roles of Vitamin C in Skin Health. *Nutrients* **2017**, *9*, No. 866.
- (6) Chen, L.; Hu, J. Y.; Wang, S. Q. The role of antioxidants in photoprotection: A critical review. *J. Am. Acad. Dermatol.* **2012**, *67*, 1013–1024.
- (7) Carr, A. C.; Maggini, S. Vitamin C and Immune Function. *Nutrients* **2017**, *9*, No. 1211.
- (8) Chaikul, P.; Sripisut, T.; Chanpirom, S.; Dittthawutthikul, N. Anti-skin aging activities of green tea (*Camelliasinensis* (L) Kuntze) in B16F10 melanoma cells and human skin fibroblasts. *Eur. J. Integr. Med.* **2020**, *40*, No. 101212.
- (9) Crisan, D.; Roman, I.; Crisan, M.; Scharffetter-Kochanek, K.; Crisan, M.; Badea, R. The role of vitamin C in pushing back the boundaries of skin aging: an ultrasonographic approach. *Clin., Cosmet. Invest. Dermatol.* **2015**, *8*, No. 463.
- (10) Garcês, A.; Amaral, M. H.; Lobo, J. M. S.; Silva, A. C. Formulations based on solid lipid nanoparticles (SLN) and nanostructured lipid carriers (NLC) for cutaneous use: A review. *Eur. J. Pharm. Sci.* **2018**, *112*, 159–167.
- (11) Zhou, W.; Liu, W.; Zou, L.; Liu, W.; Liu, C.; Liang, R.; Chen, J. Storage stability and skin permeation of vitamin C liposomes improved by pectin coating. *Colloids Surf., B* **2014**, *117*, 330–337.
- (12) Estevinho, B. N.; Carlan, I.; Blaga, A.; Rocha, F. Soluble vitamins (vitamin B12 and vitamin C) microencapsulated with different biopolymers by a spray drying process. *Powder Technol.* **2016**, *289*, 71–78.
- (13) Carità, A. C.; Fonseca-Santos, B.; Shultz, J. D.; Michniak-Kohn, B.; Chorilli, M.; Leonardi, G. R. Vitamin C: One compound, several uses. Advances for delivery, efficiency and stability. *Nanomed. Nanotechnol., Biol. Med.* **2020**, *24*, No. 102117.
- (14) Liu, H.; Jiang, W.; Yang, Z.; Chen, X.; Yu, D.; Shao, J. Hybrid films prepared from a combination of electrospinning and casting for offering a dual-phase drug release. *Polymers* **2022**, *14*, No. 2132.

- (15) Akhgari, A.; Shakib, Z.; Sanati, S. A review on electrospun nanofibers for oral drug delivery. *Nanomed. J.* **2017**, *4*, 197–207.
- (16) Calzado-Delgado, M.; Guerrero-Pérez, M. O.; Yeung, K. L. A new versatile x–y–z electrospinning equipment for nanofiber synthesis in both far and near field. *Sci. Rep.* **2022**, *12*, No. 4872.
- (17) Grosso, G.; Bei, R.; Mistretta, A.; Marventano, S.; Calabrese, G.; Masuelli, L.; Giganti, M. G.; Modesti, A.; Galvano, F.; Gazzolo, D. Effects of vitamin C on health: A review of evidence. *Front. Biosci.* **2013**, *18*, 1017–1029.
- (18) He, R.; Niu, Y.; Li, Z.; Li, A.; Yang, H.; Xu, F.; Li, F. Hydrogel Microneedle Patch for Point-of-Care Testing Based on Skin Interstitial Fluid. *Adv. Healthcare Mater.* **2020**, *9*, No. 1901201.
- (19) Guerrero-Pérez, M. O.; Patience, G. S. Experimental methods in chemical engineering: Fourier transform infrared spectroscopy-FTIR. *Can. J. Chem. Eng.* **2020**, *98*, 25–33.
- (20) Bruschi, M. L. *Strategies to Modify the Drug Release from Pharmaceutical Systems*; Elsevier, 2015.
- (21) I, M. R.; Damodharan, N. Mathematical modelling of dissolution kinetics in dosage forms. *Res. J. Pharm. Technol.* **2020**, *13*, 1339–1345.
- (22) Budiasih, S.; Jiyauddin, K.; Logavinod, N.; Kaleemullah, M.; Jawad, A.; Samer, A. D.; Fadli, A.; Eddy, Y. Optimization of Polymer Concentration for Designing of Oral Matrix Controlled Release Dosage Form. *Pharm. Biosci. J.* **2014**, *2*, 54–61.
- (23) Rehman, Q.; Akash, M. S. H.; Rasool, M. F.; Rehman, K. Role of Kinetic Models in Drug Stability. In *Drug Stability and Chemical Kinetics*; Springer, 2020; pp 155–165.
- (24) Parsa, P.; Paydayesh, A.; Davachi, S. M. Investigating the effect of tetracycline addition on nanocomposite hydrogels based on polyvinyl alcohol and chitosan nanoparticles for specific medical applications. *Int. J. Biol. Macromol.* **2019**, *121*, 1061–1069.
- (25) Saha, S.; Roy, A.; Roy, K.; Roy, M. N. Study to explore the mechanism to form inclusion complexes of  $\beta$ -cyclodextrin with vitamin molecules. *Sci. Rep.* **2016**, *6*, No. 35764.
- (26) Jiang, P.; Hao, X.; Sun, M. Characterization of Antibacterial Film Based on PVA and Clove Oil/ $\beta$ -Cyclodextrin Inclusion Complex. *Appl. Mech. Mater.* **2012**, *217–219*, 1018–1021.
- (27) Fathi-Azarbayjani, A.; Qun, L.; Chan, Y. W.; Chan, S. Y. Novel vitamin and gold-loaded nanofiber facial mask for topical delivery. *AAPS PharmSciTech* **2010**, *11*, 1164–1170.
- (28) Karim, A. A.; Tan, E.; Loh, X. J. Encapsulation of Vitamin C with its Protection from Oxidation by Poly(Vinyl Alcohol). *J. Mol. Eng. Mater.* **2018**, *5*, No. 1750013.
- (29) Moulay, S. Review: Poly(vinyl alcohol) Functionalizations and Applications. *Polym.-Plast. Technol. Eng.* **2015**, *54*, 1289–1319.
- (30) Guo, R.; Du, X.; Zhang, R.; Deng, L.; Dong, A.; Zhang, J. Bioadhesive film formed from a novel organic–inorganic hybrid gel for transdermal drug delivery system. *Eur. J. Pharm. Biopharm.* **2011**, *79*, 574–583.
- (31) Sharma, N.; Baldi, A. Exploring versatile applications of cyclodextrins: an overview. *Drug Delivery* **2016**, *23*, 729–747.
- (32) Jicsinszky, L.; Cravotto, G. Cyclodextrins in Skin Formulations and Transdermal Delivery. *J. Skin Stem Cell* **2019**, *6*, No. 102561.
- (33) Bilensoy, E. *Cyclodextrins in Pharmaceuticals, Cosmetics, and Biomedicine: Current and Future Industrial Applications*; John Wiley and Sons, 2011.
- (34) Klang, V.; Matsko, N.; Zimmermann, A. M.; Vojnikovic, E.; Valenta, C. Enhancement of stability and skin permeation by sucrose stearate and cyclodextrins in progesterone nanoemulsions. *Int. J. Pharm.* **2010**, *393*, 153–161.
- (35) Kamaly, N.; Yameen, B.; Wu, J.; Farokhzad, O. C. Degradable controlled-release polymers and polymeric nanoparticles: Mechanisms of controlling drug release. *Chem. Rev.* **2016**, *116*, 2602–2663.